DEVELOPMENT OF AN ELECTRONIC-BASED SYSTEM FOR WATER PH ANALYSIS

PAUL KIMEU NGUMBI

MASTER OF SCIENCE

(Physics)

JOMO KENYATTA UNIVERSITY OF AGRICULTURE AND TECHNOLOGY

2008

Development of an Electronic-Based System for Water pH Analysis

Paul Kimeu Ngumbi

A thesis submitted in partial fulfilment for the Degree of Master of Science in Physics in the Jomo Kenyatta University of Agriculture and Technology

2008

DECLARATION

This thesis is my original work and has not been presented for a degree in any other university.

Signature……..….. Date……

Paul Kimeu Ngumbi

This thesis has been submitted for examination with my approval as university supervisor.

Signature…… Date…….

Dr. Joseph N. Mutuku

JKUAT, Kenya

ACKNOWLEDGEMENTS

The work presented here involves direct and indirect contributions from many people. First and foremost, I wish to thank my research supervisors namely Dr. J. N Mutuku and Dr. F. O Otieno, for their valuable advice, meticulous guidance and suggestions throughout the research period. Their tireless availability for any consultations and suggestions went a long way to make this work possible. I specially thank them for their support and encouragement throughout the tough academic period. They have been my source of my inspiration.

I would also like to state my appreciation to the dean faculty of Science Prof. D. M Mulati for his support through provision of a digital oscilloscope that made my work easier. I am very thankful to all the teaching and technical staff at JKUAT Physics Department for their support throughout the research period. I also thank Mr. Sisa and Mr. Joshua, technicians at JKUAT Mechanical Engineering workshop for their assistance during the project fabrication process. I also extend special thanks to all my siblings and family at large for their total financial support even when resources were scarce. Your continued support and encouragement did a great deal to my progress.

Last but not least, I express my gratitude to my colleagues namely, Michael, Kiroe and Gachari for their brotherly cooperation during the entire course period. To all I say, thanks and God bless you.

TABLE OF CONTENTS

LIST OF TABLES

LIST OF FIGURES

LIST OF APPENDICES

ABSTRACT

The streaming potential method is commonly used for charge analysis in water treatment and the paper industry. The colloidal charge of water determines its quality. This research focused on the construction of a system for determining the electric potential in a water sample through measurement of the output voltage at different pH values. Using *AutoCAD®*, the mechanical part of the system was first drawn in 3-dimension. Design and implementation of these parts involved construction of the system cell, its housing and the cam system. The motor control circuit developed is based on pulse width modulation (PWM). The various circuits were drawn using *Circuitmaker®*. Measurements of electric potential were carried out on water sample as a function of pH in the range 2-13. The pH of the sample was adjusted with small quantities of calcium hydroxide solution, $Ca(OH)_2$ in the range 7-13, and with hydrochloric acid, HCl in the range 2-7. The results obtained showed that the output of the system varied with water pH level. In the pH range 2-6, the system output depicted a drop in potential from 33 mV to 24 mV while in the range 6-13, an increase in the output potential from 24 mV to 42 mV was noticed. From the results, the negative and positive gradient of the graph implies presence of acidic and basic media respectively. From these results, the relationship between the system output and the ionic concentration of particles in the water can be used in determining the stability of these particles hence the amount of alum needed during water treatment process. Various recommendations are given for future research especially in the automation of the system and calibration to allow measurement of other parameters such as temperature and turbidity that affect water quality.

CHAPTER 1

INTRODUCTION

1.1 BACKGROUND INFORMATION

Water is essential to life and lack of quality water for personal hygiene may result in increased transmission of water-borne diseases (Mayabi *et al.*, 2003). The quality of water partially depends on the amount of matter suspended or dissolved in it, including ions. Removal of hazardous and unwanted matter in water, such as soil particles, is facilitated through coagulation in treatment plants by combining small particles to form larger aggregates (Fredrick, 1990). Through this treatment, water may be rendered free from apparent turbidity, color, odour and bad taste.

Further, there is need for monitoring of ion charges not only in water for human consumption, but also in agricultural soils to increase plant yield (Joseph *et al.*, 1990). The cost of water treatment and quality analysis is becoming very high. To ensure proper treatment of raw water, it should first be analyzed for its chemical composition. This therefore calls for proper evaluation of water purity to enable accurate chemical dosage. There are various techniques of water quality analysis (Lyklema, 1995). One method is electrophoresis, where charged particles such as colloids move relative to the liquid they are suspended in, under the influence of an electric current field (Dukhin and Goetz, 2002). Electrophoresis occurs because particles dispersed in a fluid almost always carry an electric surface charge. An electric field exerts electrostatic Coulomb force on the particles through these charges. An electrophoresis system, in this case, consists of a capillary cell with

electrodes at either end to which a potential is applied. A second method is electro-osmosis, where the electric field causes movement of a liquid relative to a stationary charged surface (Dukhin and Goetz, 2002). It is highly applicable in soil analysis and characterization (Probstein and Ronald, 1994). These two techniques may not be highly used in water analysis since they are slow and are not very accurate (Gulo and Alexejev, 2008). A third method involves the use of streaming current detector (SCD), a technique based on generation of potential difference between two points in a flow line due to a forced flow of liquid between two solids (Chen, 2004). This potential is known as streaming potential.

Analysis of water using SCD technique is performed using the streaming current monitor, an instrument that indicates the state of chemistry in water particulate suspensions. The chemistry of water samples in this case is monitored by measuring surface charge of the particles suspended in the fluid medium (Edney, 2005). By using measured values of generated streaming current and other parameters depending on the cell geometry, zeta-potential (z), which is the electrical potential created at the solid-liquid interface due to the relative movement of particles and water (Kaya and Yukslen, 2005), can be calculated. Zeta potential in this case helps in determining properties of water suspension. It is a measure of the effective charge, meaning that it measures the ionic charge which one particle 'sees' when it approaches another particle, hence it characterizes the electrical force between approaching particles. The potential also enables identification of the different ion species and determination of their concentration. In this case, the ionic concentration is directly proportional to the potential measured. Application of the Boltzmann

distribution equation gives the type of charge species in the water sample (Williams, 1992).

Although the streaming current detector (SCD) technique is not widely used, it promises a cost-effective approach that could lower water treatment costs, improve agriculture, determine rock properties in geology, and aid research in medical and chemical physics. This is due to its simplicity in application. However, the locally available SCDs have a limited range of ±5 Ion charge units (10 units), which makes them unreliable for testing water in areas prone to higher ranges. This may lead to chemical wastage due to under-dosing or overdosing during water treatment.

1.2 JUSTIFICATION OF THE RESEARCH PROBLEM

There is need for quality water in all nations of the world, Kenya included. Much of the water consumed in Kenya is drawn from rivers and dams and in most cases is consumed raw (Mayabi *et al.*, 2003). Water drawn from most sources in Kenya has a high turbidity hence proper analysis is essential during its treatment. Consumption of such water when raw may pose health risks due to its chemical, microbiological and physical constituents. Although some of the particles suspended in water may be filtered, there are others that cannot be filtered due to their small sizes as they pass through the filter. Aggregation of such small particles is therefore essential to facilitate their settling to larger particles for easy removal. This removal of the particles reduces the risk of diseases such as cholera, typhoid, which may be caused by taking raw water.

To ensure water for consumption is properly treated, there is need to develop a mechanism to monitor its chemistry and provide a precise indication of zeta-potential to ensure correct dosing with alum. Streaming current detector (SCD) is a method that provides accurate and precise polymer dose. It also acts as an automatic dose monitoring and verification system. However, the technique is not very common in Kenya, a reason attributed to the high cost and low working range of available SCDs. By putting this problem into account, there is a need to design a water quality control system based on a fabricated sensor hence lowering its cost from Kshs.150,000 to approximately Kshs.50,000. In addition, it will help in determination of the chemical dosage during water turbidity and pH control. Since the available SCDs have a low range, this system is designed to allow measurement of a greater range of values from sensor output through optimization of the annular spacing, where adsorption takes place.

1.3 OBJECTIVES

The general objective of this research project is to develop an electronic-based system for use in water streaming potential measurement.

Specific objectives are:

i. To develop a motor controlled reciprocating piston cell for generating streaming potential.

ii. To design a circuit to process low streaming current signals.

iii. To calibrate the system to measure streaming potential.

CHAPTER 2

LITERATURE REVIEW

2.1 ELECTROKINETICS AND COLLOIDAL SYSTEMS

2.1.1 Water Treatment Process

Water for public supply can be obtained from underground sources or from surface sources. Treatment process is done through the steps below (WHO, 2007).

Step 1: Preliminary Treatment

The collected water is first screened to remove suspended and floating debris, such as leaves or branches. It involves pre-chlorination, pre-conditioning, storage, screening, pumping and containment

Step 2: Coagulation and Flocculation

This removes colloidal particles which cannot be removed by sedimentation or filtration alone. Flocculation is a process which clarifies the water. Clarifying involve removing any turbidity or colour so that the water is clear and colourless. Clarification is done by causing a precipitate to form in the water which can be removed using simple physical methods. Coagulants or flocculating agents that may be used include Iron (III) hydroxide or Aluminium hydroxide.

Step 3: Sedimentation

Allows suspended solids sink to the bottom under the force of gravity and form sediments for easy removal. The sludge collected in any sedimentation tank in the

water treatment process is disposed. The cost of treating and disposing of the sludge can be a significant part of the operating cost of a water treatment plant. The sedimentation tank may be equipped with mechanical cleaning devices that continually clean the bottom of the tank.

Step 4: Filtration

In filtration, the partially treated water is passed through a medium such as sand or anthracite which retains the fine organic and inorganic material making the water clean. Particles which can not pass through sand filters are removed using synthetic polymeric membranes at a high pressure.

Step 5: Disinfection

Disinfection is accomplished both by filtering out harmful microbes and also by adding disinfectant chemicals in the last step in purifying drinking water. Water is disinfected to kill any pathogens which pass through the filters. Drinking water is further treated to remove components such as nitrates. However, for groundwater aeration may be done to remove carbon dioxide and iron for which may be dissolved.

Step 6: Distribution

The water from service reservoirs is distributed by a network of pipes of various sizes, laid beneath the streets, pavements and verges of our towns and cities.

2.1.2 Water quality standards

The quality of water for public use is monitored by various bodies. The Kenya Bureau of Standards (KEBs) and the National Environmental Management Authority (NEMA) are the main bodies that oversee water quality in Kenya while the World Health Organization (WHO) and the Environmental Protection Agency (EPA) are some of the international bodies that set and regulates public water quality standards. Some of the set standards are as shown in table 2.2 below (LeChevallier, 2004).

Table 2.1: Water quality parameters

Microbial parameters	
Total caliform bacteria	Maximum Accepted Concentration (MAC) 0 organisms per 100mL
Fecal caliform bacteria	MAC 0 organisms per 100mL
Inorganic parameters	
pH	Desirable range : 6.5-8.5
Conductivity	< 250 µS/cm
Fluorine	MAC 1.5 mg/L
Copper	MAC 2.0 mg/L
Iron	Desirable: = 0.3 mg/L
Chlorine	Desirable: < 250 mg/L
Lead	MAC 0.01 mg/L
Manganese	Desirable: = 0.05 mg/L
Sodium	Desirable : = 200 mg/L
Nitrate (as nitrogen)	MAC 10 mg/L

Physical parameters	
Colour	Desirable: 15 mg/l Pt-Co
Hardness	Desirable: 150-500 mg/L
Dissolved oxygen	Desirable: < 75% of the saturation concentration
Turbidity	Desirable: < 5 nephelometric turbidity unit (NTU)

2.1.3 Electrokinetic measurements

The term electrokinetics is derived from two terms: electro, which refers to electricity and kinetics, which refers to motion. Therefore, electrokinetics refers to electrically induced motion. Development towards improved understanding of equilibrium properties of confined fluids has included both theoretical and computational methods in statistical mechanics (Bryk *et al.*, 2000). The most widely used geometries have been the spherical and cylindrical configurations and the obtained results have shed light on a number of molecular phenomena underlying experimental observations. For cylindrical geometry, the adsorption takes place in an 0annulus (pore) formed between two cylindrical surfaces. Adsorption in this case refers to the process of collecting soluble substances that are in the solution, on a suitable interface (liquid and a gas, a solid or another liquid) and allows measurement of colloidal charge between the given interfacial surfaces.

The electrokinetic charge of a particle can be measured in a number of ways. Two common methods are the applied electric field and the induced electric potential. The applied electric field method involves measurement of relative mobility of the solid or liquid phase such as electrophoresis. Motion of the charged particles (colloids)

under the influence of an electric field is observed and the potential required to achieve certain particle mobility and the induced electric potential measured. In the induced electric potential method, the potential developed between two electrodes as a result of forced movement of the particles (colloids) in the solution is measured, for example, sedimentation potential.

2.1.4 Size of colloidal particles

The size of the various components involved in coagulation can vary by many orders of magnitude as shown in the table below (Dixit *et al.*, 2002).

Table 2.2: Size of the various components involved in coagulation

Colloidal Systems	Diameter (Å)
Color bodies	50-1,000
Inert colloids (clay, silt, inorganic salts)	1,000-30,000
Emulsions	2,000-100,000
Bacteria	5,000-100,000
Algae	50,000-8,000,000
Cations (Na^{+}, Ca^{2+}, Mg^{2+}, Al^{3+})	1-2
Polyelectrolyte (100,000-15,000,000 M.W)	250,000-40,000,000
Electrical double layer	5-100
Water	4

Coagulation is primarily directed towards colloidal fractions, which gives water its turbidity. Turbidity in water is caused by suspended particles in the range of

approximately 0.01µm to 100µm in size. The larger fraction of the suspended particles can easily be removed by settling. The smaller particles, with sizes less than 5µm are referred to as colloidal particles (or colloids) and have extremely slow settling velocities and cannot be practically removed by settling. The behavior of colloidal particles is strongly influenced by their electrostatic charge. This colloidal charge comes as a result of the uneven surface characteristics of the particles and in most solids is negative, particularly the alumino-silicate clay typically suspended in surface water (Zarbov *et al.*, 2004). The charges on the particles will repel each other and prevent significant flocculation from occurring. Neutralizing this charge is the main purpose of coagulation. However, just considering the particle charge as an electrostatic surface charge is oversimplification since the whole solution must have a neutral charge and a layer of water containing ions of opposite charge surrounds each colloid. For practical purposes, the surrounding ions must also be taken into consideration since they are inseparable from the particles.

2.1.5 Stability of colloids

Some colloids are stable indefinitely while others are not. Colloids that are stable indefinitely are energetically or thermodynamically stable; they are termed as reversible colloids (Novich and Ring, 1984). Examples include the ordered structures from soap and detergent molecules called micelles, proteins, starches, large polymers, and some humid substances. Colloids that are not stable indefinitely coagulate hence are termed as irreversible. Some irreversible colloids coagulate slowly and others rapidly hence referred to as kinetic colloids. Kinetically stable colloids are irreversible or thermodynamically unstable suspensions that coagulate at

a very slow rate while kinetically unstable colloids coagulate rapidly. Coagulation process therefore increases the rate or kinetics at which particle aggregates.

The important forces occurring between the particles include the van der-waals forces, electrostatic forces caused by the adsorbed molecules, and the hydrodynamic forces. Forces from the adsorbed polymers operate when these molecules are present. They are frequently added to water treatment plants. Natural organic matter (primarily humic substances) adsorbs on colloidal particles and has been recognized as contributing to the stability of the particles in many natural waters.

2.1.6 Origin of colloid stability

An important factor in the stability of colloids is the presence of surface charge. It develops in a number of different ways, depending on the chemical composition of the medium (concentration of ions in the raw water in this case) and the colloids. Regardless of how it is developed, this stability must be overcome if these particles are to be aggregated into larger particles with enough mass to settle easily. Surface charge develops most commonly through preferential adsorption, ionization, and isomorphous replacement. For example, oil droplets, gas bubbles or other chemically inert substances dispersed in water will acquire charge through preferential adsorption of anions, particularly hydroxyl ions (OH^-). In case of substances such as proteins or micro-organisms, surface charge is acquired through the ionization of the carboxyl and amino groups. This can be represented as:

$$R_{NH_2}^{COO-} \quad At\ high\ pH$$

$$R_{NH_{3+}}^{COOH} \quad At\ low\ pH \qquad (2.1)$$

$$R_{NH_{2+}}^{COO-} \quad At\ isoelectric\ point\ (IEP)$$

Where R is the bulk of the solid.

2.2 THEORETICAL DESCRIPTION OF THE SYSTEM SENSOR

The streaming current detector (SCD), also called the streaming current monitor (SCM), sensor or analyzer was first introduced in 1966 (Walker *et al.*, 1996). Various attempts have been made at modeling the SCD. The original approach was based on a simplified triangular fluid velocity profile within an annulus (Gerdes, 1966a). Later work used a more appropriate fluid profile model (Elicker *et al.*, 1992). Recently, inertial effects were considered within the annulus. It was found that for the geometries used in typical SCDs, the earlier approximate solutions produced very similar results to the more complete model in which the output current was seen to be a function of sensor geometry (Walker *et al.*, 1996). These models assume that the surface of the piston (sensor) is completely and uniformly coated by the colloidal particles and by any coagulant in the solution in a representative manner. This is not necessarily a valid assumption and probably goes along way towards explaining the poor predictive abilities of this theory (Dentel *et al.*, 1989a; Borron *et al.*, 1994). Gerdes (1966a) acknowledged the poor predictive abilities of this type of model and the existence of double-equilibrium theory, which states that, the charge on a particle surface is the result of equilibrium between the ions on the surface and in the solution. The charge on the two different types of surfaces, which are both in

equilibrium with the same liquid, will be related to one another in a way that depends on their equilibrium constants. Using this theory, it is only possible to predict that any change in the colloidal system that changes zeta-potential will change streaming current in the same direction.

In the recent years the SCD has become widely used in water treatment industries as a method of continuous, on-line monitoring and of controlling coagulant dosage. This is evident at Warragul water treatment plant in Australia where a Milton Roy SC 5200 SCD model was developed to control the chemical dosing and color removal (Ablett, 2003). Other water treatment works employing SCD technique include; Regina Wastewater Treatment Plant (RWWTP) in Canada and Umgeni Water Plant in South Africa (Krishnamurthy and Viraraghavan, 2005). The latter uses SCDs for turbidity removal and coagulant dosage control (Nozaic *et al*, 2001). It is also used in other applications where colloidal charge is to be altered by a controlled chemical dosage.

The device sensor comprises a piston that reciprocates vertically within a cylindrical housing (Fig. 2.1) that is closed at the bottom. The cylinder is fitted with a pair of electrodes located at axially opposite ends of the annular space between the piston and the cylinder. Above the narrow annular zone is a reservoir of water containing the charged colloidal material to be characterized. The water may be tested by immersion of the sensor in a batch sample or by provision of a flow-through line for continuous sampling in an on-going process. Fluid carrying charged colloidal

material (and associated counter-ions) is drawn into and out of the annular space as the piston moves up and down.

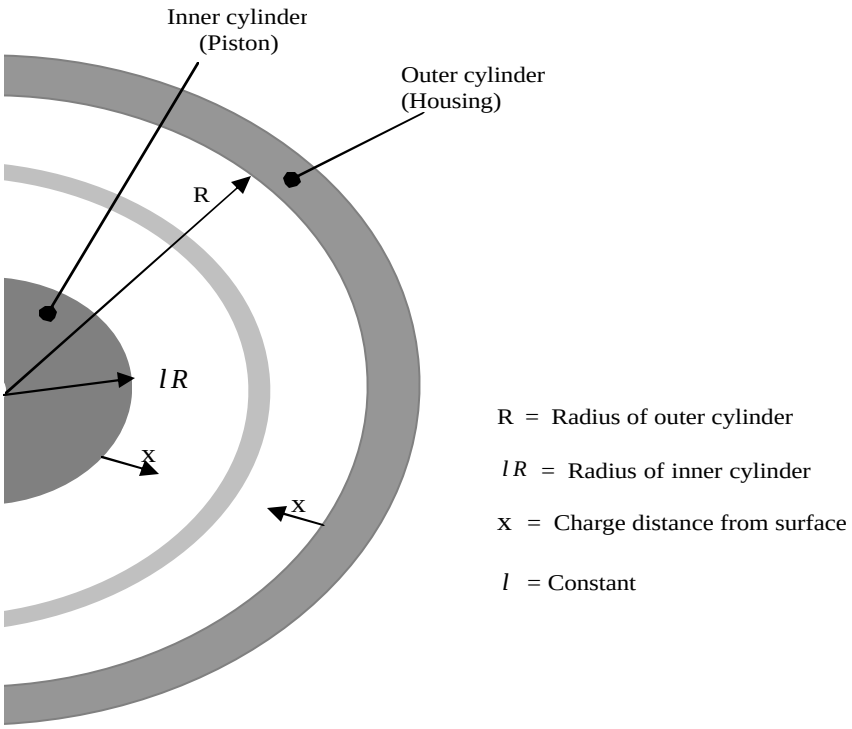

Figure 2.1: Schematic diagram of halved cross-section of SCD cylindrical sensor model

By considering this cylindrical model, much has been done to improve the quality of the SCDs for various applications in Biology, Chemistry, and Geophysics such as monitoring ion charges in fluids, soils and rocks as well as any other related areas of research. The principle of capillary action is applied in the operation of the SCD (Williams, 1992). To investigate the electro-osmosis through an annulus the electric potentials and flow velocity profiles are obtained by solving the linearized Poisson-

Boltzmann equation. Poisson equation describes the relationship between the potential and charge, as given by equation below.

$$\frac{d^2y}{dx^2} = -\frac{r}{e} \tag{2.2}$$

Where x= distance from the surface (m), y = electric potential (V), r = charge density (C/m^2) and e = permittivity of the medium. The charge density of the ions in the double layer is;

$$r = e\sum z_i n_i \tag{2.3}$$

Where e is the electronic charge (1.6 x 10 $^{-19}$ C), z_i and n_i are the charge and concentration of the i^{th} ion, respectively. The concentration of the cations (n_+) and anions (n_-) in the double layer is given by the Boltzmann distribution,

$$n_+ = n_o \exp\left[-\frac{z_i y}{kT}\right]$$
$$n_- = n_o \exp\left[\frac{z_i y}{kT}\right] \tag{2.4}$$

The Poisson-Boltzmann equation therefore becomes

$$\frac{d^2y}{dx^2} = -\frac{e}{e}\sum_i z_i n_o \exp\left[\frac{z_i e y}{kT}\right] \tag{2.5}$$

Where n_o= total ionic concentration (ions/m^3), T = Temperature (K) and k= Boltzmann Coefficient (1.38x10 $^{-23}$ J K). For a simple case of monovalent ions, analyzing double layer limits, zeta potential (z) is calculated from the Helmholtz-Smoluchowski (H-S) equation (Williams, 1992). This is given by

$$z = \frac{h u}{e_r e_o} \tag{2.6}$$

Where h is the viscosity of the solution, e_i is the relative permittivity of the solution, and e_o is the permittivity of vacuum ($e_o = 8.85 \times 10^{-12} Fm^{-1}$). The Helmholtz-Smoluchowski equation assumes that the particle size is much greater than Debye length (k^{-1}), which is a parameter having units of length that characterises the thickness of the diffuse layer (Terabe *et al.*, 1980; Kaya and Yukselen, 2005).

$$k^{-1} = \left[\frac{e k T}{8p n_o z_i^2 e^2} \right]^{1/2} \tag{2.7}$$

Research on electro-osmotic flow through an annulus shows that there exists a net flows even for zero area-averaged surface charge density due to the curvature differences between the inner and outer walls (Tsao, 2000). The flow direction was found to be determined by the sign of the charge on the inner cylinder (This is the opposite for a capillary with the same sign of the net charge). The relationship between l, R and the inverse Debyes length (k^{-1}) is as shown in inequalities below.

$$\lambda R >> \kappa^{-1}$$

$$(1-\lambda) >> \kappa^{-1} \tag{2.8}$$

$$\kappa^{-1} >> R$$

Where l = constant ($0.9079 < l < 0.9831$), R = radius of the outer cylinder, lR = radius of the inner cylinder (Tsao, 2000).

A parallel plate microchannel for streaming potential measurement was later implemented using the principle of electric double layer and improved slope technique (Erickson *et al.*, 2000). More researches on measurement of zeta potential by using the streaming current technique have been recently conducted (LeChevallier, 2004; Fuzhi *et al.*, 2006).

Lianguang *et al.*, (1999) worked on the mechanism of electro-osmotic flow by looking at the Silica surfaces as characterized by presence of several types of silanol groups (SiOH), which are weakly acidic in character. In contact with an aqueous solution, some of the silanol groups got ionized and caused the surface to be negatively charged and an electric double layer (EDL) developed within it. The EDL refers to the space charge region that exists at the interfacial boundary of two different phases (Fig. 2.2). They found the thickness of the diffuse EDL to be in the order of Debye length, k^{-1} (equation 2.7). When an electric field was imposed tangentially to a surface, the electric force acted upon the spatial distribution of ions within the diffuse layer causing unilateral movement of the ions towards the oppositely charged electrode. During their migration, these ions drag the surrounding bulk solvent molecules resulting in an overall movement of the solution relative to the stationary charged surface, a phenomenon referred to as the electro-osmotic flow. Smoluchowski (Timothy and Davis, 1999) developed the first theoretical description of the electro-osmotic flow. The EDL or electro-kinetic radius, and the surface zeta potential determine the electro-osmotic flow when an electric potential is applied across a capillary.

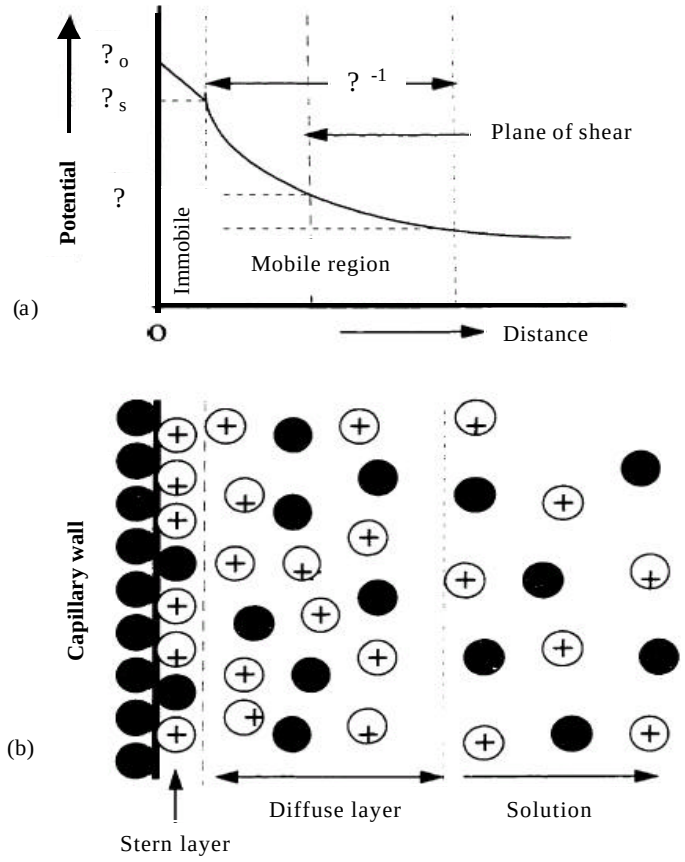

Figure 2.2: A schematic diagram of the electrical double layer that develops at the charged interface of the wall

According to Timothy and Davis (1999), the governing equation of the electro-kinetic phenomena under influence of applied pressure and potential gradient across capillaries filled with electrolyte basically involve Smoluchowski formula

$$z = \frac{36\,p\,h}{e} \times U \times 10^{7} \qquad (2.9)$$

Where $U = vL/V$ = Electrophoretic Mobility, v = speed of Particle, V = Voltage (V) and L = Electrode distance.

2.3 DC / AC STREAMING POTENTIALS

Although the streaming potential phenomenon has been studied for many years and has been applied in diverse fields as already mentioned, much research has been done in direct current (DC) streaming potential but little has been done in frequency-dependent streaming potentials in capillaries. Models to compare direct current and alternating current streaming potentials for a capillary were developed in which the EDL is simply represented by a parallel plate capacitor (Helmholtz model) or an exponentially decaying charge distribution (Gouy-Chapman model) (Reppert *et al.*, 2001). Combining these two models provides a more accurate model that takes into account finite ion size where a fixed layer (stern layer) exists at this surface. This is the inner layer with thickness about that of a hydrated ion from the surface. A diffuse layer in which there is a shear plane that represents the limit to which the counter ions can be swept from the surface by fluid motion extends from the fixed layer into the bulk solution (Gouy-Chapman diffuse layer). Ions within the shear plane move with the particles while those outside it move independently (Sundstron and Klei, 1979). This is the stern model of EDL. The closed plane to the surface at which fluid motion can take place is called the slipping plane. The slipping plane has a potential defined as zeta potential (ζ), which is characteristic of the solid and liquid that constitute the bulk of the liquid phase (Fig. 2.2).

The streaming potential occurs when relative motion between the two phases displaces ions tangentially along the slipping plane by viscous effects in the liquid just as mentioned (Walker *et al.*, 1996; Timothy and Davis, 1999; Prieve, 2004). This displacement of ions generates convection current and has properties similar to

an ideal current source. For this capillary, in steady-state equilibrium, the convection currents (I_{conv}) and the conduction currents (I_{cond}) are found to be equal. For the AC streaming potentials, the basic electro-kinetic principles are the same as those of the DC streaming potential except the hydrodynamic part of the solution where a sinusoidal pressure of the AC case replaces the constant pressure of the DC case. These two models have the following form:

$$z = \frac{I}{k.s.w.e.f(r,R)} \tag{2.10}$$

Where: I = average current magnitude, s = piston stroke length, w = motor cycles per second, e = dielectric constant of solution, z = zeta potential, r = piston radius, R = chamber radius (Fig. 2.1), k = electronics gain constant and $f(r,R)$ is a function of the annulus shape which depends on the model used (Walker, 1996; Edney, 2005).

The modern colloidal-science theories provide no discussion of how, or at what rate, the measurement surfaces take on the zeta-potential characteristics of the sample. If equilibrium does exist between the charge on the particles in solution and the charge on the measurement surfaces then it would influence the rate at which measured SC responds to changes in coagulant dosage (Edney, 2005). It is quite possible to calibrate an SCD so that it reads directly in units of zeta-potential over a limited range or in units matching another SCD parameter. However, it will not stay calibrated when in continuous use as conditions of the surface changes with time (Dentel *et al.*, 1989; Elicker *et al.*, 1992).

Considering the various works done on the streaming current detector, Lechintec Company of South Africa in the year 2000 developed an instrument that could measure zeta potential by use of the streaming current detector cell (http://www.users.iafrica.com). Later in 2002, Rank Brothers company of South Africa devised an instrument, which they called charge analyzer II (CAII) (http://www.rankbrothers.co.uk/. 2002). This instrument applied the above principle to perform water titration. The two instruments consisted of a reciprocating piston detector cell and could measure the streaming current to the range of −5 to +5 Ion Charge units. More theoretical work has been done on the applications of SCDs by LeChevallier (2004) and Fuzhi (2006). Their results showed that ion concentration in water greatly influences the value of zeta potential obtained from an SCD but failed in providing a practical way of calculating this quantity for water with high colloidal particles. This therefore called for more research on instrumentation for streaming potential measurement especially in such cases where turbidity is high. This was the driving force for this research.

CHAPTER 3

METHODOLOGY

3.1 INTRODUCTION

This chapter discusses the procedure for the development of a device that determines the streaming potential in water through charge analysis. It will determine the surface charge of the suspension by streaming current technique. With the optimized annular spacing, the output of this device provides a higher range compared to the output of the existing SCDs. The system consists of three main parts; the streaming current detector cell, the mechanical part and the electronic circuitry that function as described in the section below.

3.2 SYSTEM DESIGN

The device components stated above detects the electric potential generated at the annular space as water is forced into this space by the piston motion when the motor is switched on. The signal is hence amplified by the electronic circuit for detection and analysis. Each of these parts is briefly discussed below.

3.2.1 Streaming Current Detector cell

The streaming current sensor cell is shown in Fig. 3.1. It comprises a motor and cell mounting bracket (incorporated with a drive motor) and the measuring cell.

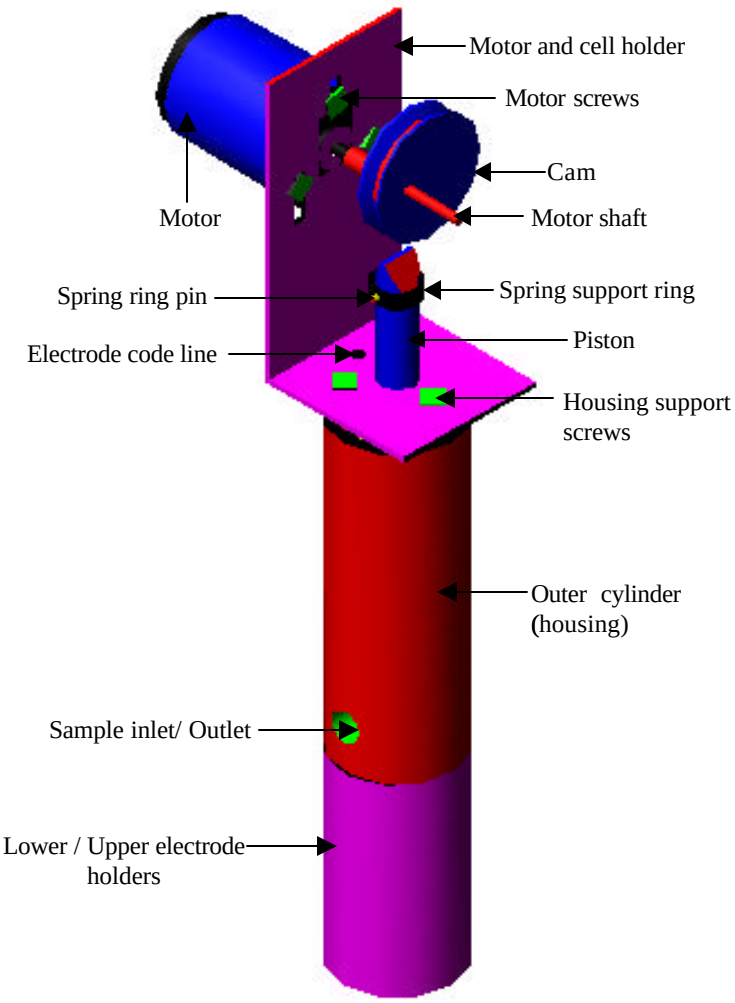

Figure 3.1: A diagram of the developed water quality control system

3.2.1.1 Device sensor

The sensor (cell) for the device in Fig. 3.1 comprises a piston that reciprocates vertically within a cylindrical housing closed at the bottom. This piston is as shown in Fig. 3.2a. The cylinder is fitted with a pair of electrode rings located axially in the annular space between the piston and the cylindrical housing. To allow the electrodes to be well positioned within the annulus, the housing has two electrode supporters as

shown in Fig. 3.2b, with measurements as indicated in the appendix (Fig. B4). Water is streamed into the annular space through an inlet of diameter 10 mm as in Fig. 3.1 by dipping the cell in a water container such as a jar.

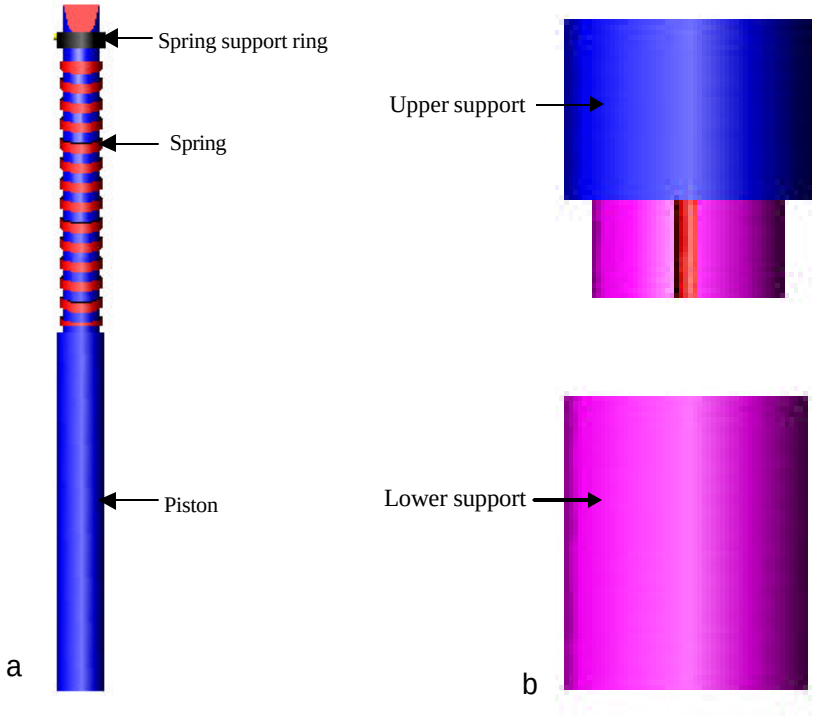

Figure 3.2: (a) Sensor piston, (b) Electrodes support

Water streaming into and out of the annular space occurs as the piston oscillates axially inside the cylinder at a specified speed generating an alternating current at the electrodes attached to the ends of the cylinder. Flowing liquid will induce charge accumulation, insulating surfaces over which they flow. These charges become momentarily immobilized on the surfaces of the piston and the cylinder.

The movement of these charged layers produces a difference in potential (zeta potential), and the alternating current induced by the moving charges is known as the streaming current and is directly related to the charge on the particles. The amount of charge that accumulates in the liquid depends on the rate at which the ions diffuse towards the interface and on the liquid resistivity (?). The streaming current is, however constant over time.

The piston and its housing are developed from a nylon material since it is easily machinable to required shape and texture, and not prone to rusting. Polyethylene could do as well. The water was first passed through a sieve to ensure that before entering into the annular space it is free from particulate matter of a solid nature greater than 0.1 mm in size. This prevents wear and scratches on the piston due to friction.

The relationship between the internal diameter of the housing and that of the piston is given by equation (2.8). The external diameter of the cell housing is 41.40 mm. Although this diameter is not critical for the functioning of the instrument, the size is convenient for use with various water containers used in homes such as water jugs where the instrument housing is dipped during its operation. By setting the internal diameter of the sensor housing as 33.10 mm, from equation (2.8), the piston diameter is determined as 14 mm. From its geometry, other dimensions of the piston are as shown in the appendix (Fig. B3).

Equation 2.8 ensures that l is in the range $0.9079 \text{ mm} < l < 0.9831 \text{ mm}$. From l, the optimal value of the annular spacing (Fig 3.1) of 0.15 mm was determined, and is the value used in the research. The annulus is important in the design of the system since it determines the amount of water that is in the system at any particular moment.

Conductivity in water can be tested by setting the circuit as in Fig. 3.3, with the ammeter in the microampere scale. The current flow in this circuit is very small and is due to the presence of H^+ and OH^- ions produced when a few of the water molecules dissociate and recompose spontaneously. As more salt is added to the water and stirred, its conductivity increases. This is due to presence of more ions, specifically Na^+ and Cl^- ions in the water.

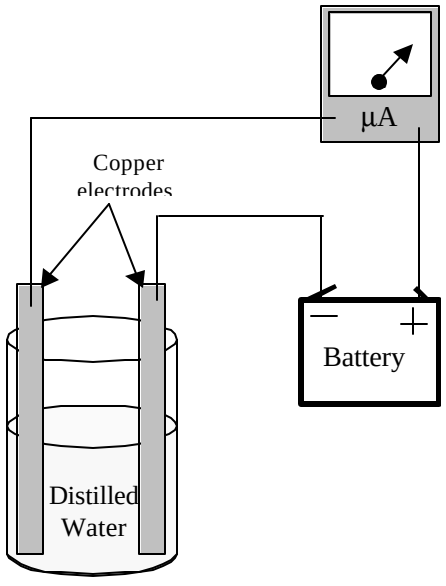

Figure 33: Testing conductivity in water

Similarly, concentration of ions in water colloids is directly proportional to the cell potential (zeta-potential) hence generated streaming current. In this case, platinum was used to design the electrodes since it is inert. The current developed due to the potential induced between two electrodes by the forced movement of the charged particles past the electrodes is then processed externally via an electronic circuitry.

The designed ring electrodes are 15.40 mm in diameter. This allows easy movement of the piston within the housing. The two electrodes are placed 27.20 mm apart within the housing and are connected to an external electronic circuitry which allows for signal processing and analysis. This electrode separation is not critical in the overall system performance.

3.2.1.2 Estimation of the device annular dimension

The annular spacing is crucial for the operation of this device since it determines its working range. Its dimensions were determined by comparing different sets of cylinders. Two sets of the outer cylinder of internal diameter 15.4 mm and 15.1 mm were made while for the piston, three sets of external diameter 15.0 mm, 15.1 mm and 15.3 mm were made. In order to obtain different sets of annular spacing, two sets were paired and data obtained was as shown in table 3.2 below where R is the internal diameter of the outer cylinder while l R is the piston diameter.

Table 3.1: Variation of the annular dimensions

R (mm)	lR (mm)	$R - lR$ (mm)	$\frac{R - lR}{2}$ (mm)
15.40	15.30	0.10	0.05
15.50	15.30	0.20	0.10
15.40	15.10	0.30	0.15
15.50	15.10	0.40	0.20
15.50	15.00	0.50	0.25

3.2.1.3 Motor and cell housing holder

To allow the system to be well aligned, an 'L' shaped steel metal sheet is designed as shown in Fig. 3.4. The slots in the metal sheet make it possible for the piston to reciprocate freely within the annulus as the motor cam rotates. The motor slots are designed to allow the cam to be positioned directly over the piston upper end, which is wedge-shaped acting as cam follower. The slot also enables setting of the piston position for free maximum lift depending on the spring length.

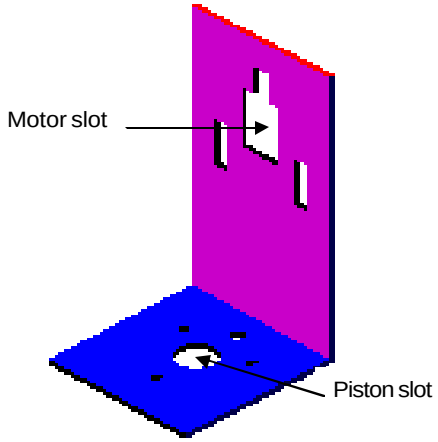

Figure 3.4: Motor and cell housing holder

3.2.2 Signal processing electronic circuitry

Processing of generated signal is an important aspect of this system. The voltage output from the cell is very low; hence it is first amplified. This part consists of an instrumentation amplifier, rectifier and a filter circuit for adjusting the output to smoothen and eliminate noise in form of AC signals (Fig. 3.5). This circuit provides a continuous reading that characterizes the magnitude of charge in the sample being tested. The gain of the circuit is given by equation 3.1 below.

$$G = \frac{100\ k\Omega}{R_G} + 1 \tag{3.1}$$

Where G is the amplifier gain while R_G is the gain resistor. Since the value of R_G in this circuit is $100\ k\Omega$, then the circuit has a gain of 2. The device output potential is hence given by;

$$V_{out} = V_{in}\ G \tag{3.2}$$

Where V_{in} is the potential from the electrodes while V_{out} is the amplified output potential.

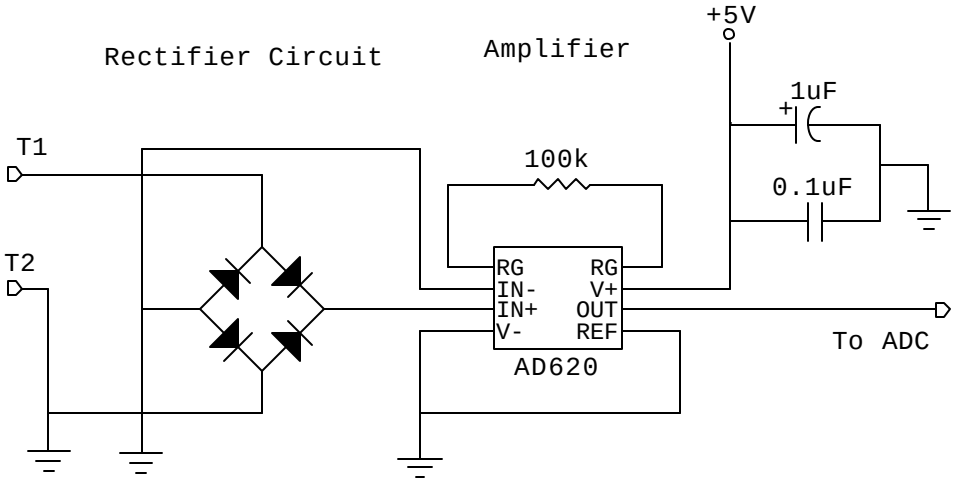

Figure 3.5: A schematic diagram of the signal processing circuit

3.2.3 Mechanical drive component

This includes a 12-volt DC. motor and its drive and speed control circuit.

3.2.3.1 Cam system

The cam system is shown in Fig. 3.6. An eccentric cam, which is a disc having its axis of rotation positioned 'off centre' is used to convert the shaft rotary motion into reciprocating motion. As the cam rotates, the follower, which in this case is the piston, rises and falls at a constant rate. The rise is facilitated by a spiral spring of free length 90 mm. The follower is fine pointed and accurately traces the outline of the cam creating a simple harmonic motion. As the cam turns, driven by the rotary motion, the cam follower traces the surface of the cam transmitting its motion to the piston, which in effect reciprocates past the two electrodes.

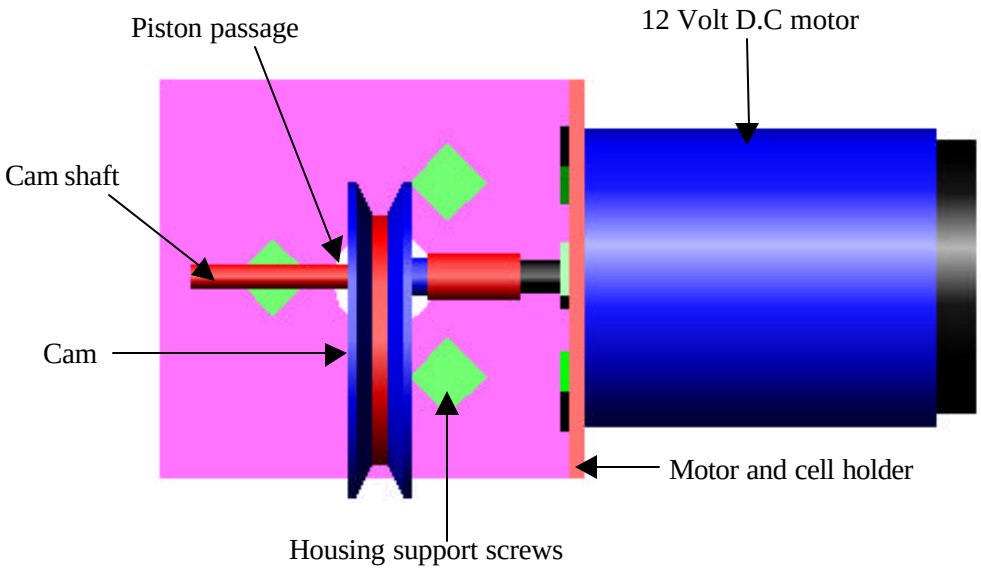

Figure 3.6: DC motor and cam system

3.2.3.2 Determination of piston lift

The cam radius is 20.00 mm. It has a groove of depth of 3.85 mm hence the working radius is 16.15 mm. Piston lift (L) is calculated from the equation;

$$L = H - h \tag{3.3}$$

Where $H = r + x, \quad h = r - x, \quad R$ = cam radius, r = working radius and x = distance of motor shaft off-centre.

$$\begin{aligned} L &= (r + x) - (r - x) \\ &= (16.15 + 8.00) - (16.50 - 8.00) \\ &= 24.15 - 8.15 \\ &= 16 \ mm \end{aligned} \tag{3.4}$$

This lift can be used in determination of the amount of water that enters or leaves the annulus at each piston stroke.

3.2.4 Motor speed control system

The motor speed control system is shown in Fig 3.7. The PWM control works by switching the power supplied to the motor on and off very rapidly. The DC voltage is converted to a series of a square-wave signal, alternating between fully on (nearly 12V) and zero, giving the motor a series of power "kicks". If the switching frequency is high enough, the motor runs at a steady speed due to its fly-wheel momentum. By adjusting the duty-cycle of the signal (modulating the width of the pulse, hence the 'PWM') i.e., the time fraction it is "on", the average power can be varied, and hence the motor speed.

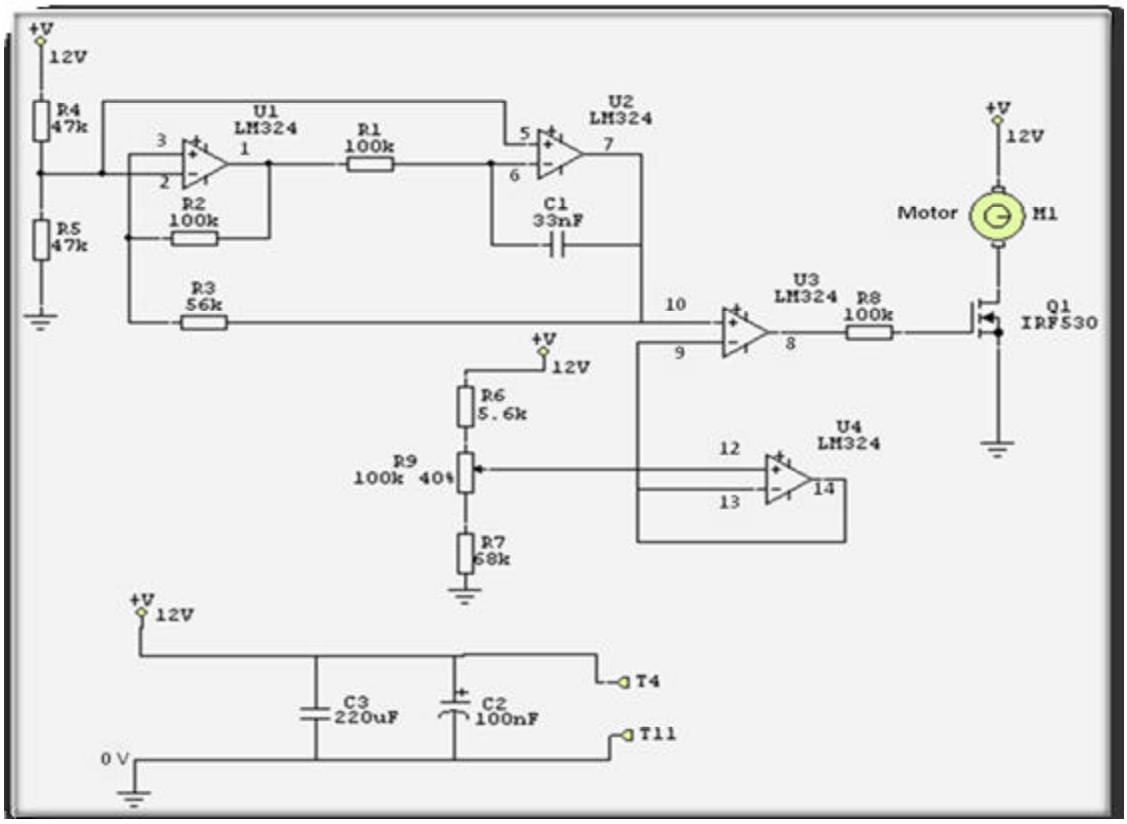

Figure 3.7: Motor speed control system design circuit diagram

In operation of this circuit, an oscilla tor is used to generate a triangular or sawtooth waveform as shown in Fig. 3.8. At low frequencies the motor speed tends to be jerky, at high frequencies the motor's inductance becomes significant and power is lost. A potentiometer is used to set a steady reference voltage (V_{ref}). A comparator compares the sawtooth voltage with the reference voltage. When the sawtooth voltage rises above the reference voltage, a power transistor is switched on. As it falls below the reference, it is switched off. This gives a square wave output to the motor. When the potentiometer is adjusted to give a high reference voltage, the

sawtooth never reaches it, so the output is zero. With a low reference, the comparator is always on, giving full power.

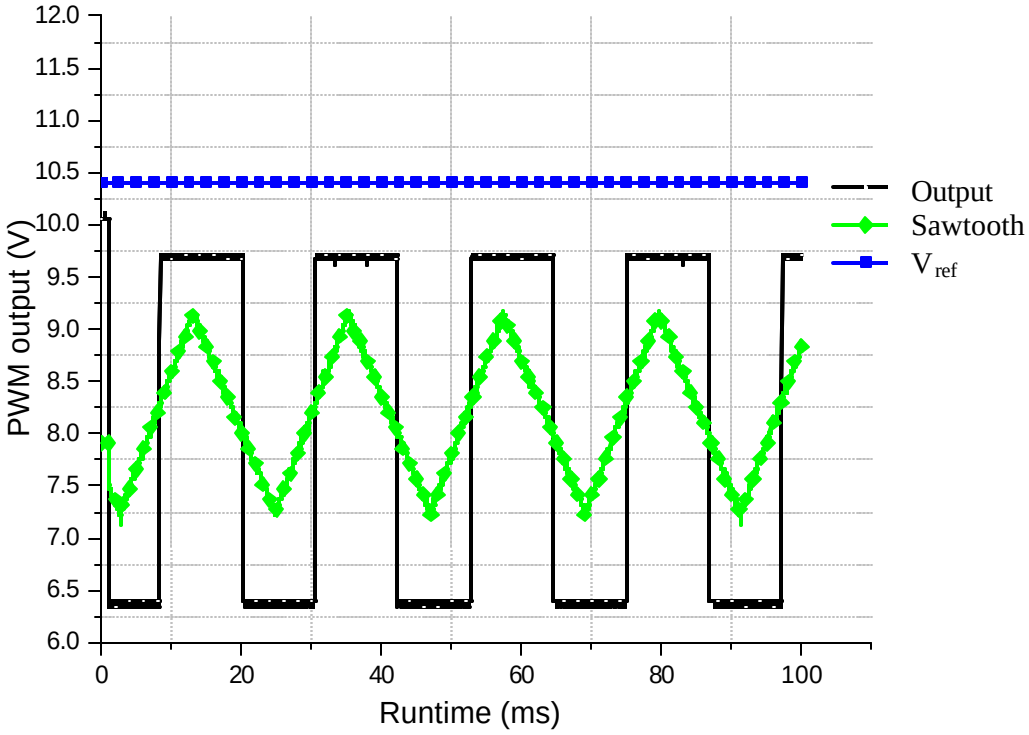

Figure 3.8: Comparison of output signals to the reference signal

This circuit uses the LM324, a 14-pin DIL IC containing four individual op-amps on a single power supply. From the circuit (Fig 3.7), a sawtooth is generated with two of the op-amps (U1 and U2), configured as a Schmitt Trigger and Miller Integrator respectively, and a third one (U3) being used as a comparator to compare the sawtooth with the reference voltage and to switch the power transistor. The fourth op-amp is used a voltage follower to buffer the reference potential divider. A sawtooth wave coming from the output of U1 is shown in Fig. 3. 8. The amplitude swings between 6.3 V and 9.8 V on a 12 V supply as shown in Fig. 3.9.

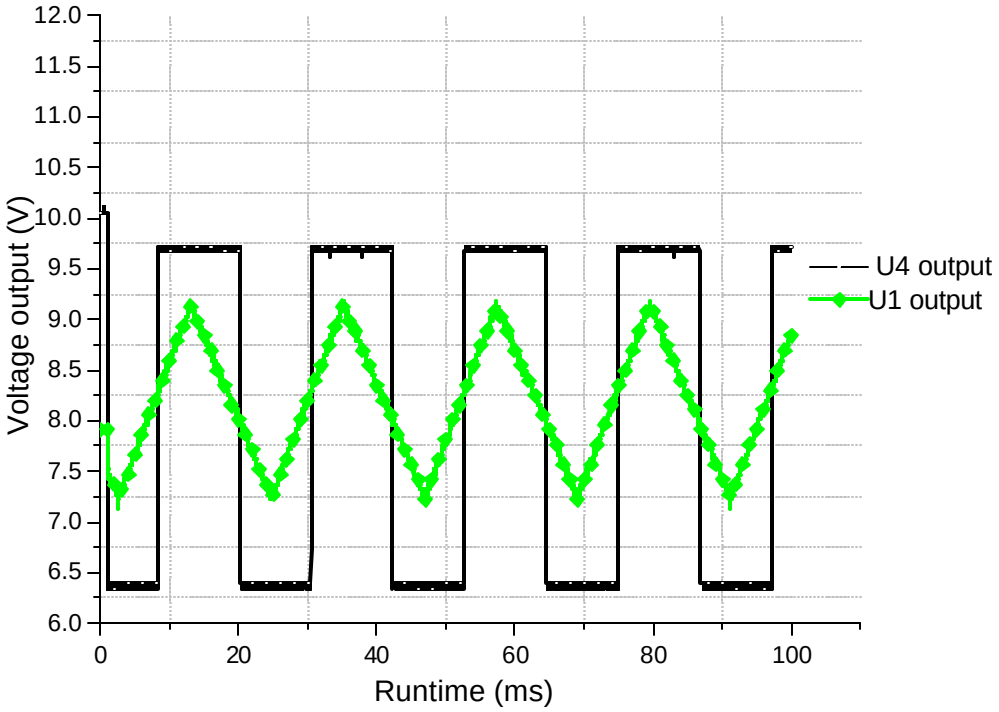

Figure 3.9: Comparison between U1 and U4 outputs

In the circuit (Fig 3.7), the reference voltage is designed to apply a level ranging from 6V to 7.5V to the comparator. There are two capacitors across the +12V and 0V power supply lines, a 220 uF 16V electrolytic and a 100 nF ceramic type. These remove the noise on the supply, particularly useful with long leads. For the switching transistor, MOSFET IRF530 was used. This transistor is easy to find, not expensive, and can carry high current (up to 12A). Most n-channel MOSFETS can also work provided they have adequate current handling ability. Using the n-channel MOSFET, R8 can be a link wire between the op-amp output and the gate. Due to the radio frequency interference (RFI) generated by the MOSFET when switching, damping was done using a low-value resistor (100Ω). Any value of R8 between 10Ω and 100Ω worked well

The advantages of this circuit design are that the output transistor is either on or off, not partly on as in with normal regulation, so less power is wasted as heat. With a suitable circuit there is little voltage loss across the output transistor, so the top end of the control range gets nearer to the supply voltage than linear regulator circuits and the full power pulsing action runs the motor at much lower speed than the equivalent steady voltage.

CHAPTER 4

RESULTS AND DISCUSSION

4.1 ESTIMATION OF OPTIMUM ANNULAR SPACING

Since the annular spacing is important in the operation of this system, Table 4.1 shows the data used in estimation of its optimum value. The data was obtained from measurement of the system output at three different water pH values 2, 7 and 12 for different sets of annular spacing. Figure 4.1 shows the relationship between the system output (mV) for the different annular sizes. Comparing the results at pH values 2, 7 and 12, the graphs show a common trend. The system output is higher at lower value of the annular spacing and decreases as the spacing increase. An optimum value of 0.15 mm, a point at which the three graphs show a nearly constant output regardless of further increase in the annular spacing. This point is taken as the optimum value, hence used in determining the dimensions of the piston and housing.

Table 4.1 : System output at different annular spacing and pH values

Annular spacing (mm)	System output at pH 2 (mV)	System output at pH 7 (mV)	System output at pH 12 (mV)
0.05	43	38	50
0.10	38	31	44
0.15	33	22	39
0.20	34	21	38
0.25	34	21	37

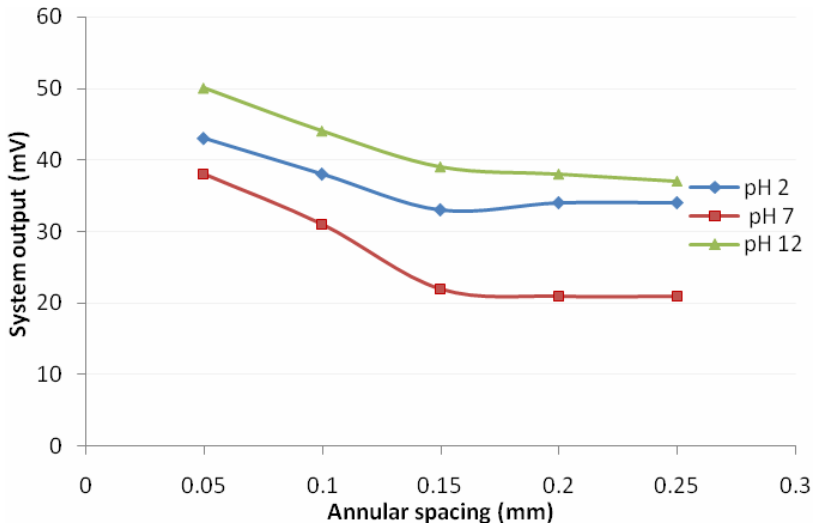

Figure 4.1: System output under different annular spacing and pH values

4.2 SYSTEM OUTPUT

Figure 4.2 shows the output signal from the electrodes when the system is running. This signal is sinusoidal and has amplitude of 1 mV.

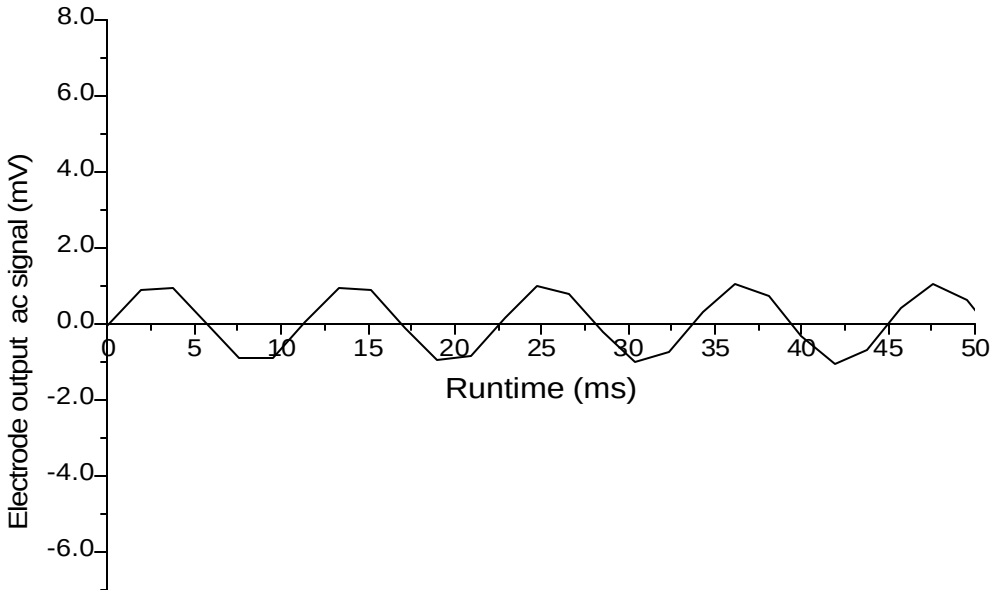

Figure 4.2: Raw electrode output ac signal

When the output signal in Figure 4.2 was passed through the amplifier circuit, the output appeared as shown in Figure 4.3. This is an indication of the system ability to detect potential difference in the water sample being tested. This amplified signal is essential in case of system automation.

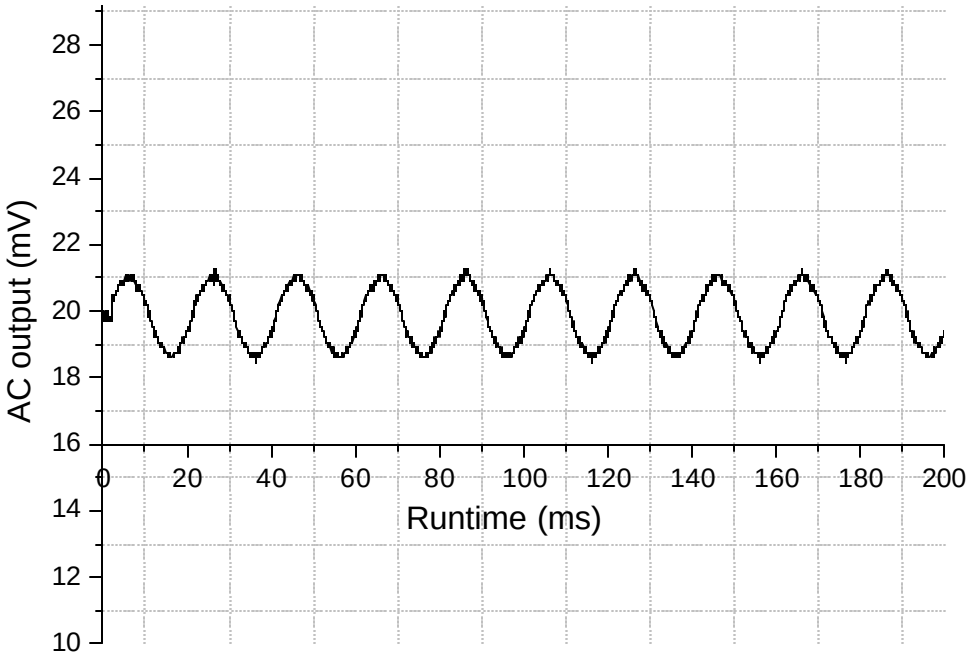

Figure 4.3: Amplified electrode output ac signal

Table 4.2 shows data obtained for different pH values from the system when the piston is in motion and when it is not in motion.

Table 4.2: System output under different pH values

pH Value	System under static piston (mV)	System under piston motion (mV)
2	34.0	34.5
3	28.0	32.0
4	26.0	31.0
5	24.5	29.5
6	22.5	28.0
7	20.5	25.0
8	22.0	31.0
9	31.5	39.0
10	35.0	41.5
11	37.0	42.5
12	39.0	43.0
13	40.0	42.0

Figure 4.4 shows the system output at different water pH values. Comparing table 4.1 and table 4.2, the output potential at pH value 2, 7 and 12 are approximately equal when the annular spacing is 0.15 mm. This shows a sense of reproducibility of the system results. From the graph, the absolute system output is high at the extreme sides of the pH line. This is attributed to the large number of sodium ions (Na^+), hydrogen ions (H^+), hydroxyl ions (OH^-) and chloride ions (Cl^-). The gradient of the curve is negative at low pH values. This is an indication of the presence of large

number of positive ion (Na^+ and H^+) compared to the negative ions (OH^- and Cl^-) in the water sample. On the other hand, the curve has a positive gradient at higher pH values, an indication of presence of a large number of negative ions (OH^- and Cl^-) compared to the positive ions (Na^+ and H^+) in the sample. At pH between 6 and 7, each of the two graphs attains a minimum point. At this point the graphs have a gradient of zero. This minimum value determines the isoelectric point, where the colloidal system is least stable. At this point, the ionic concentration of particles in the water sample is very low hence the pH is neutral. Generally, if more alkali is added to the water sample, the particles in it tend to acquire more negative charge. If acid is added, then a point is reached where the charge will be neutralized. Further addition of acid cause a build-up of positive charge hence change in the gradients of the curves.

Comparing the two curves (Fig. 4.4), the system output is higher when the motor is running. This is attributed to the effect of the piston motion. This increases the surface area for adsorption at the annulus due to the complete coverage of the piston and housing surfaces by the charged particles.

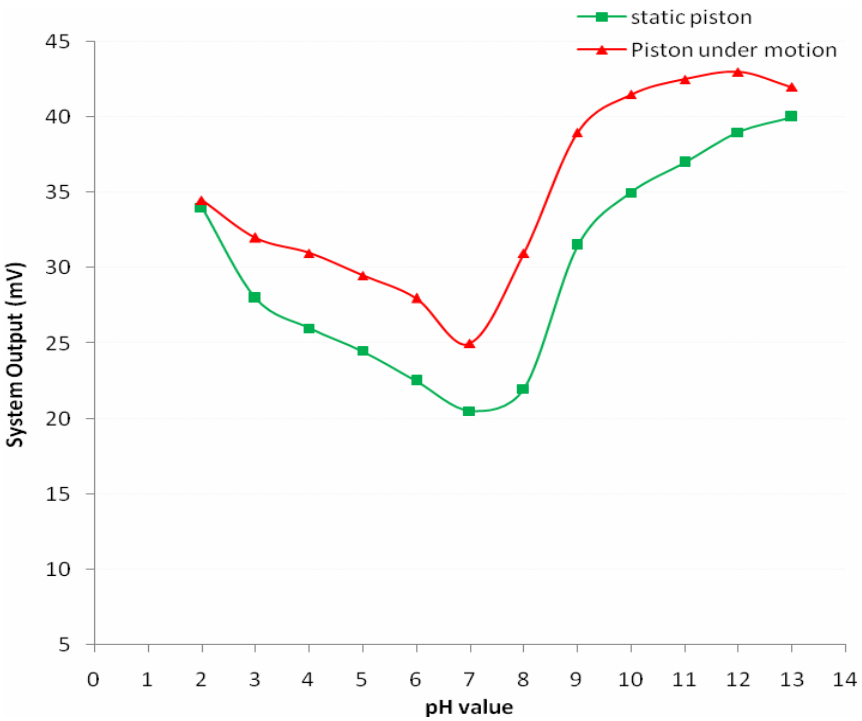

Figure 4.4: System output under different pH values

The magnitude of the system output gives an indication of the potential stability of the colloidal system. If all the system output potential is large, then it implies the particles will repel each other and there is dispersion stability. On the other hand if the output system potential is low, then there is no much force to prevent the particles coming together hence there is dispersion instability.

Figure 4.5 gives the average system output along a pH line. It can be seen that if the dispersion pH is below 2 or above 9, there is sufficient charge to confer stability. However if the pH of the system is between 2 and 9 the dispersion may be unstable. This is the most likely to the case at pH 6 (isoelectric point) where the system output is lowest (24 mV). Such critical points were also achieved by Guichet *et al.*, (2006),

where in modification of streaming potential in the pH range 4 to 12 the isoelectric point was reached at pH 7.

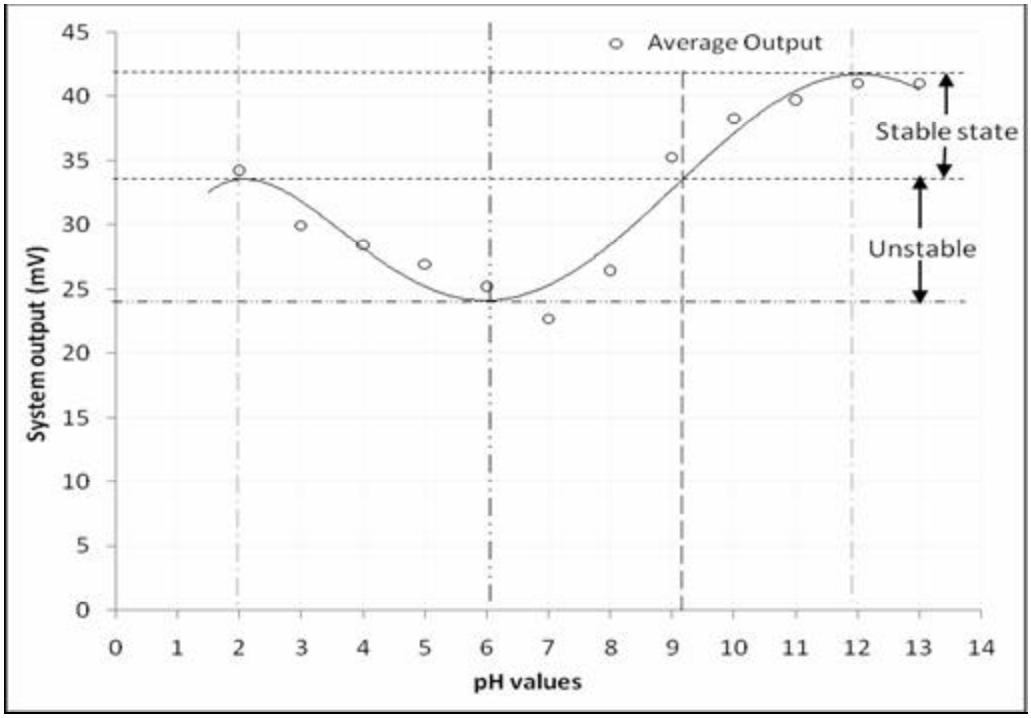

Figure 4.5: Average system output

CHAPTER 5

CONCLUSION AND RECOMMENDATIONS

5.1 CONCLUSION

From the obtained data, the optimum value for the annular spacing in streaming potential generation is 0.15 mm. The signal processing circuit had a gain of 2 which gave a reliable amplification for the output potential. By considering the results obtained, the system output is found to be affected by the change in the ionic charge of particles in water sample. This is evident from the measured difference in the system output at varied pH values. The neutral point reached at pH value between 6 and 7 provided a dividing line for the stable and unstable aqueous dispersions which in this case is taken as 24 mV. The absolute values of the system output in the pH values lower than 6 indicated presence of acidic condition in the tested sample while those values in the pH values higher than 6 indicated presence of basic condition in the sample.

From Figure 4.5, the system shows stable state is reached at an absolute output of 33 mV, a value obtained at a pH range between 2 and 9. In the unstable state, particle in water sample have no forces to prevent them from coming together and there exist dispersion instability. This allows the colloidal particles in the sample to coagulate during water treatment hence can be easily removed. On the other hand, in stable state particles will repel each other hence there exist dispersion stability. This makes it difficult for them to coagulate during water treatment. From this information the magnitude of the system output is determined by the degree of stability of the

colloidal particles in water sample hence provides information on the amount of forces holding these particles together. This principle can be employed in determination of the chemical dosage in water treatment since the amount of chemical needed to neutralize the ionic concentration of a sample may be determined using this system.

5.2 RECOMMENDATIONS

In future modification of this project, the motor control and signal processing circuits can be specified earlier in the design process to allow more time for verification and testing. Due to the improvement in technology, the efficiency of the system can be improved through automation using microcontrollers. A chemical inlet system could also be incorporated in this system so that when water treatment process is being done, chemical being used could automatically add to the water. In addition, inclusion of digital display readout in the system would also make the instrument more user friendly. The system could also be calibrated to accurately and automatically measure various parameters such as temperature, microbiological and physical conditions that affect quality of water consumed.

REFERENCES

Ablett, L. (2003). Use of a Streaming Current Detector at Warragul Water Treatment Plant. 66th Annual Water Industry Engineers and Operators' Conference, Eastbank Centre–Shepparton, pp. 112-118.

Alshawabkeh, A. N. (2001). Handout Prepared for Short Course Basics and Applications of Electrokinetic Remediation: Department of Civil and Environmental Engineering. Federal University of Rio de Janeiro. p. 27.

Bryk, P., Sokolowski, S., Pizia, O. and Sokolowska, Z. (2000). Adsorption of fluids in pores formed between two hard spheres. *Journal of Colloid and Interface Science*, **229**, pp. 526-533.

Chen, J. (2004). Factors affecting interactions of polyelectrolytes during charge analysis. A PhD dissertation, North Carolina State University. Raleigh. pp. 118-200.

Chibowski, E., Hotysz, L. and Szczes, A. (2003). Time dependent changes in zeta potential of freshly precipitated calcium carbonate. *Colloids and Surfaces A: Phys. Eng. Asp*. **222** Issue 1-3, p. 41.

Dentel, S. K. and Kingery, K. M. (1989). Using the Streaming Current Detector in Water Treatment, *Journal of American Water Works Association*, **81**, p. 443.

Dixit, S., Crain, J., Poon, W. C., Finney, J. L. and Soper, A. K. (2002). Molecular segregation observed in a concentrated alcohol-water solution. *Nature* ***416***, pp. 829-832.

Dukhin, A. S. and Goetz, P.J. (2002). "Ultrasound for characterizing colloids". Particle sizing, Zeta potential, Rheology. Elsevier, the Netherlands. pp. 2-8.

Dunn, W. E. (2003). Fundamentals of signal processing, instrumentation and control: Speed control of a dc electric motor, pp. 2-24.

Edney, D. B. L. (2005). Control and Optimization of Coagulant Dosing in Drinking Water Treatment. Ph.D. Thesis. University of Auckland. pp. 5-41.

Elicker, M. L., Resta, J. J., Hunt, J. W. and Dentel, S. K. (1992). A Fundamental Basis for Use of the Streaming Current Detector, *Proc. 1992* American Water Works Association Annual Conference. (Vancouver), pp. 3-12.

Erickson, D., Li, D. and Werner, C. (2000). An improved method of determining zeta potential and surface conductance. *Journal of Colloid and Interface Science.* **232**, pp. 186-197.

Fair, G. M., Geyer, J. C. and Okun, D. A. (1968). Water and Wastewater Engineering, **2**, Wiley, New York, pp. 25-118.

Fredrick, W. P. (ed.), (1990). American Water Works Association: Water quality and treatment. McGraw-Hill, New York. USA, pp. 121-324.

Fuzhi, L., How, T.Y. and Kwok, D. Y. (Jul. 2006). An improved method for determining zeta potential and pore conductivity of porous materials. *Journal of Colloid and Interface Science*, **299** Issue 2, pp. 972-976.

Gerdes, F. W. (1966a). A New Instrument-The Streaming Current Detector. Analysis Instrumentation, **4**, pp. 181-198.

Gerdes, F. W. (1966b). Apparatus for Measuring Charge Condition within a Solution. US Patent number 3 **368** 145.

Guichet, X., Jouniaux, L. and Catel, N. (2006). Modification of streaming potential by precipitation of calcite in a sand–water system: laboratory measurements in the pH range from 4 to 12. *International Journal of Geophysics.* **166**, pp. 445–460.

Gulo, D. L. and Alexejev, O. L. (2008). Determination of the electrical conductivity and the electroosmotic transfer in the concentrated dispersions on the basis of the cell theory of the electroosmosis. 42 Vernadsky blvd., 252142 Kyiv, Ukraine, pp. 1-12.

http//www.rankbrothers.co.uk/. (2002). Charge analyzer II, Rank Brothers Ltd. England. February, 2007.

http://www.users.iafrica.com/l/le/lechtech/index.htm, (2004). Ion charge analyzer operating and instruction manual, January, 2007.

Hubbe, M. A. (2006). Sensing the Electrokinetic Potential of Cellulosic Fibers. *Journal of BioResources, **1**(1):* pp. 116-149.

Joseph, A. (1990). Rationale of water quality standards and goals. American Waterworks, pp. 143-186.

Kaya, A. and Yukselen, Y. (2005). Zeta potential of clay minerals and quartz-contaminated by heavy metals. *Canadian Journal of Geotechnology,* **42**, pp. 1280-1289.

Krishnamurthy, S. and Viraraghavan, T. (2005). Chemical Conditioning for Dewatering Municipal Wastewater Sludge. Faculty of Engineering University of Regina, Saskatchewan Canada. Energy Sources, **27**, pp. 113–122.

LeChevallier, M. W. and Kwok-Keung, A. (Eds.), (2004). World Health Organization, Water Treatment and Pathogen Control: Process Efficiency in Achieving Safe Drinking Water, IWA Publishing, London, UK. pp. 288-300.

Lianguang, H., Harrison, J. D. and Masliyah, J. H. (1999). Mechanism of Electroosmotic Flow. *Journal of Colloid and Interface Science*, **215**, pp. 300-312.

Lyklema, J. (1995). Fundamentals of Interface and Colloid Science, Academic Press, London, UK. **2**, pp. 1-5.

Mayabi, A. O., Mwachiro, E. C., Gachanja, A. and Maina, A. (2003). Water quality and its improvement for rural household supply in Kitui District, Kenya. Proceedings of the international civil engineering conference on sustainable development in the 21st century, Nairobi, Kenya, pp. 362-368.

Newcomer, B. (1999). Investigating the Effect of Texture on the Relative Benefit of Electro-osmosis in Soil Remediation. A sword-billed hummingbird project. pp. 2-15.

Niehof, R. A. and Loeb, G. I. (1972). "The surface charge of particulate matter in sea water," Limnology Oceanography, **17**, p. 7.

Novich, B. E. and Ring, T. A. (1984). Colloid Stability of Clays Using Photon Correlation Spectroscopy. *Journal of Clays and Clay Mineral*, **32**, No. 5, pp. 400-406.

Nozaic, D. J., Freese, S. D. and Thompson, P. (2001). Long-term experience in the use of polymeric coagulants at Umgeni Water, Pietermaritzburg, South Africa. Water Science and Technology: Water Science, **1** No.1, pp. 43-50.

Prieve, D. C. (2004). Changes in zeta potential caused by a dc electric current for thin double layers. *Colloids and Surface A: Phys. Eng. Asp* ., **250** Issue 1-3, pp. 67-77.

Probstein, R. F. (1994). *Physicochemical Hydrodynamics.* New York: Wiley, pp. 3-7.

ProTech Technical Report. (2005). Automated Monitoring and Dosage of Polymer Coagulants in Storm water Treatment using a Streaming Current Detector. pp. 1-6.

Reppert, P. M., Morgan, F. D., Lesmes, D. P. and Laurence, J. (2001). Frequency-dependent streaming potentials. *Journal of Colloid and Interface Science*, **234**, pp. 194 – 203.

Sundstron, D. W. and Klei, H. E. (1979). Wastewater Treatment: prentice Hall, New York, USA. pp. 25–124.

Sze, A., Erickson, D., Ren, R. and Li * D. (2003). "Zeta-potential measurement using the Smoluchowski equation and the slope of the current–time relationship in electro osmotic flow", Journal of *Colloid and Interface Science*, **261**, pp. 402–410.

Terabe, S., Yamamoto, K. and Ando, T. (1980). Streaming current detector for a reversed-phase liquid chromatography. *Canadian Journal of Chemistry*, **59**, pp. 1531-7.

Timothy J. J. and Davis, E. J. (1999). An analysis of electrophoresis of concentrated suspensions of colloidal particles. *Journal of Colloid and Interface Science*, **215**, pp. 397-408.

Tsao, H. K. (2000). Electro-osmotic Flow through an annulus. *Journal of Colloid and Interface Science*, **255**, pp. 247- 250.

Walker, C. A., Kirby, J. T. and Dentel, S. K. (1996). The Streaming Current Detector: A Quantitative Model. *Journal of Colloid and Interface Science*, **182**, pp. 71–81.

World Health Organization (2007). Combating waterborne diseases at the household level part 1. pp 1-10.

Williams, R. A., (ed.), (1992). Characterization of process dispersions, Butterworth-Heinemann, Oxford, pp. 3-18.

Yufeng, X. and Deng, Y. (2003). Characterization of charge neutralization reaction in aqueous solution using the membrane separation method. *Journal of Colloid and Interface Science*, **264** Issue 1, pp. 271.

Zarbov, M., Schuster, I. and Gal-or. (2004). "Methodology for selection of charging agents for electrophoretic deposition of ceramic particles", *Journal of Materials Science*, **39**, pp. 813– 817.

APPENDIX I

The contents in this section include some photographs and *AutoCAD*® diagrams of the system.

A. PHOTOGRAPHS

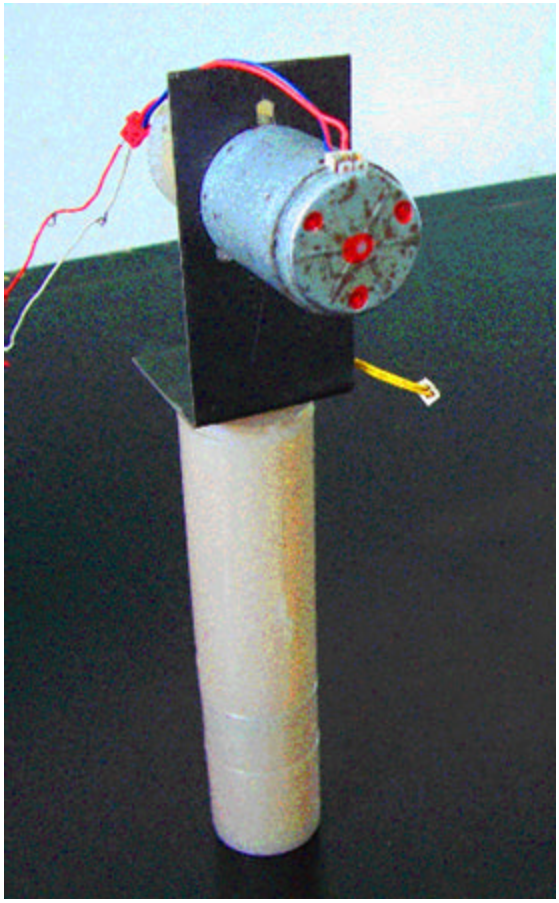

Figure A1: Motor and cell assembly

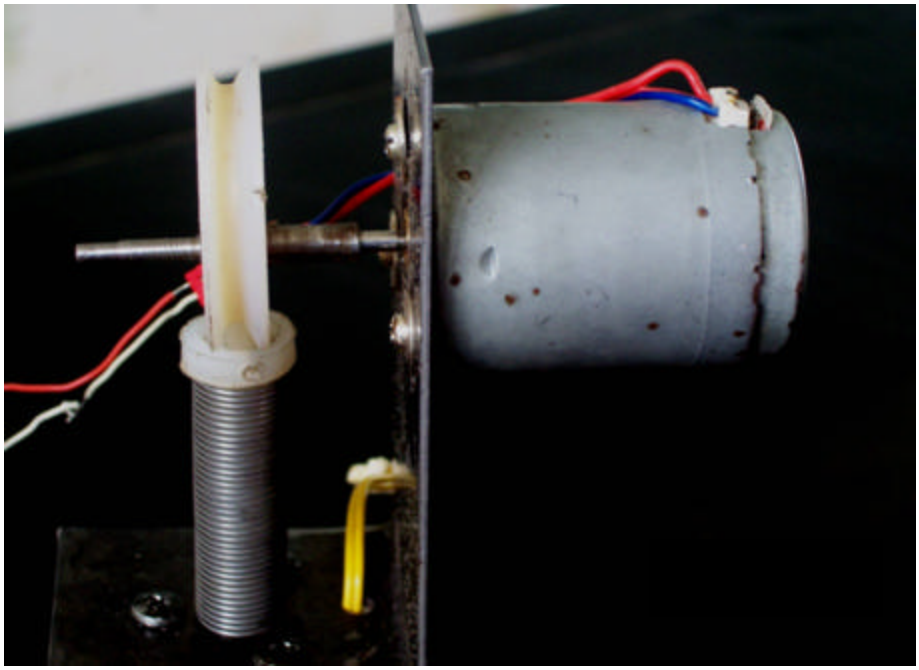

Figure A 2: Motor and cam assembly

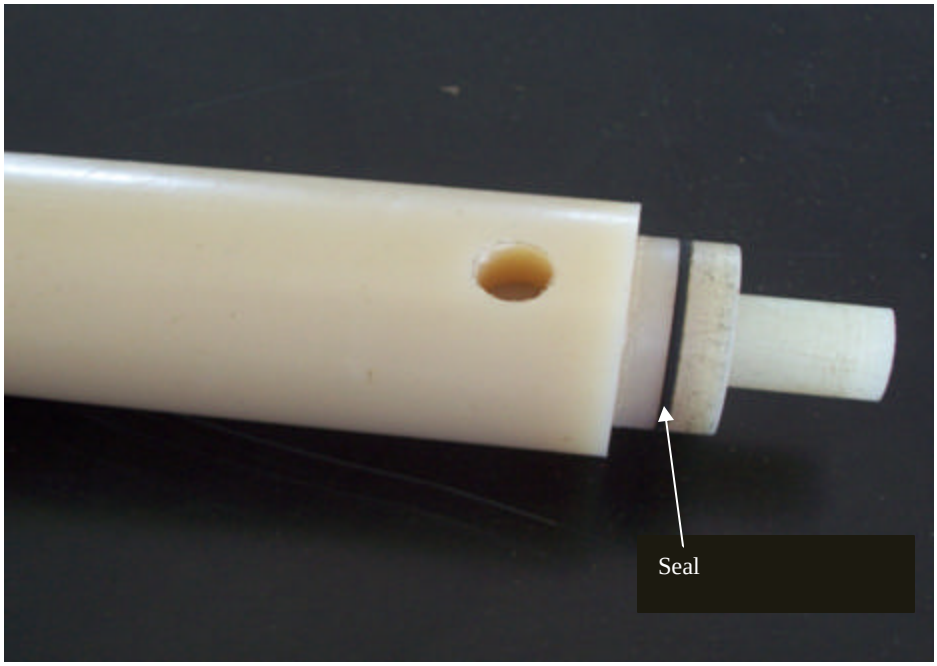

Figure A 3: Water inlet point, piston and electrodes position

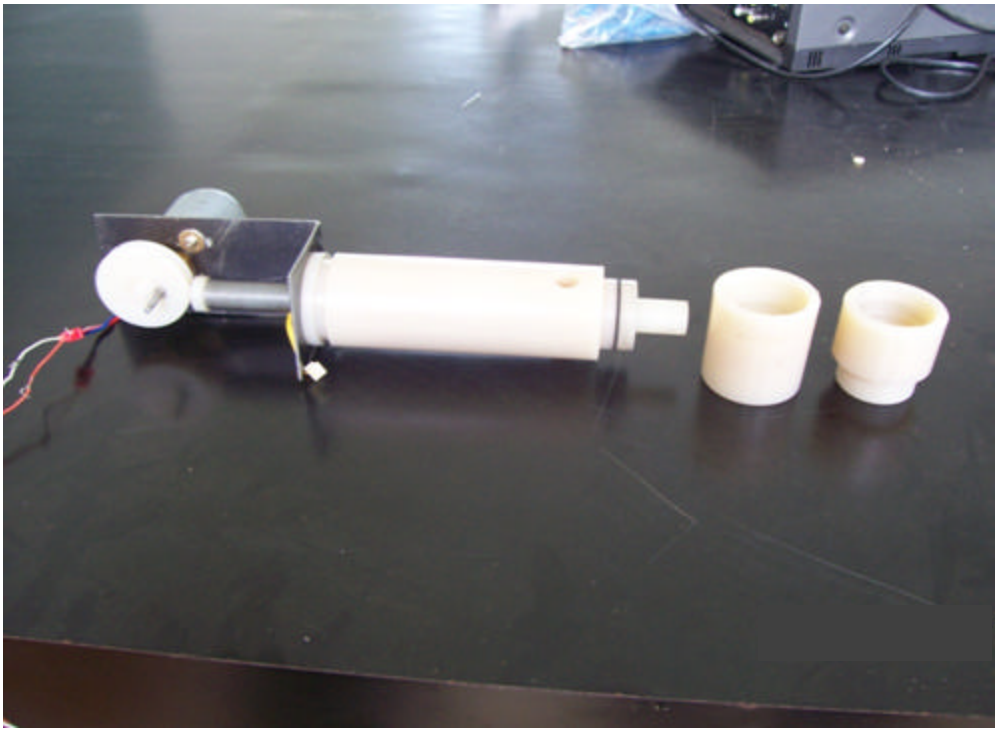

Figure A 4: Portions of the casing which holds electrodes

B. *AutoCAD*® DIAGRAMS

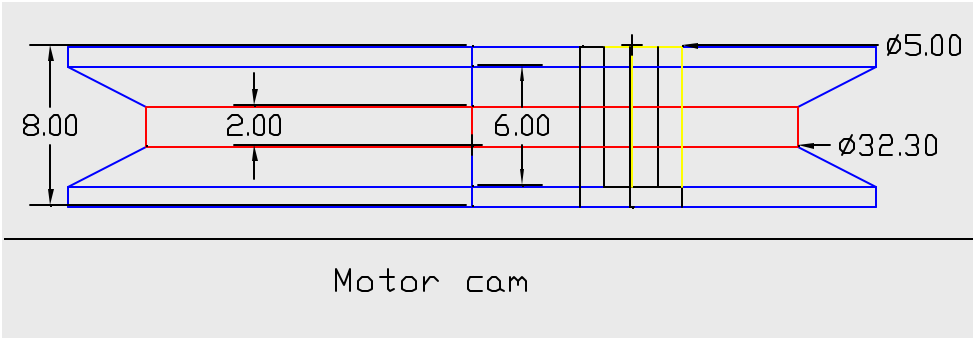

Figure B 1: Cam dimensions

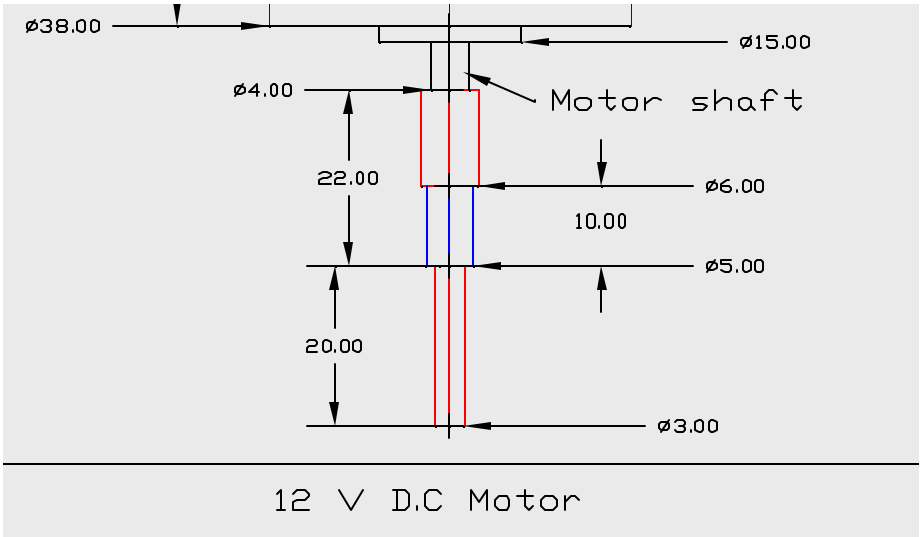

Figure B 2: Cam-shaft dimension

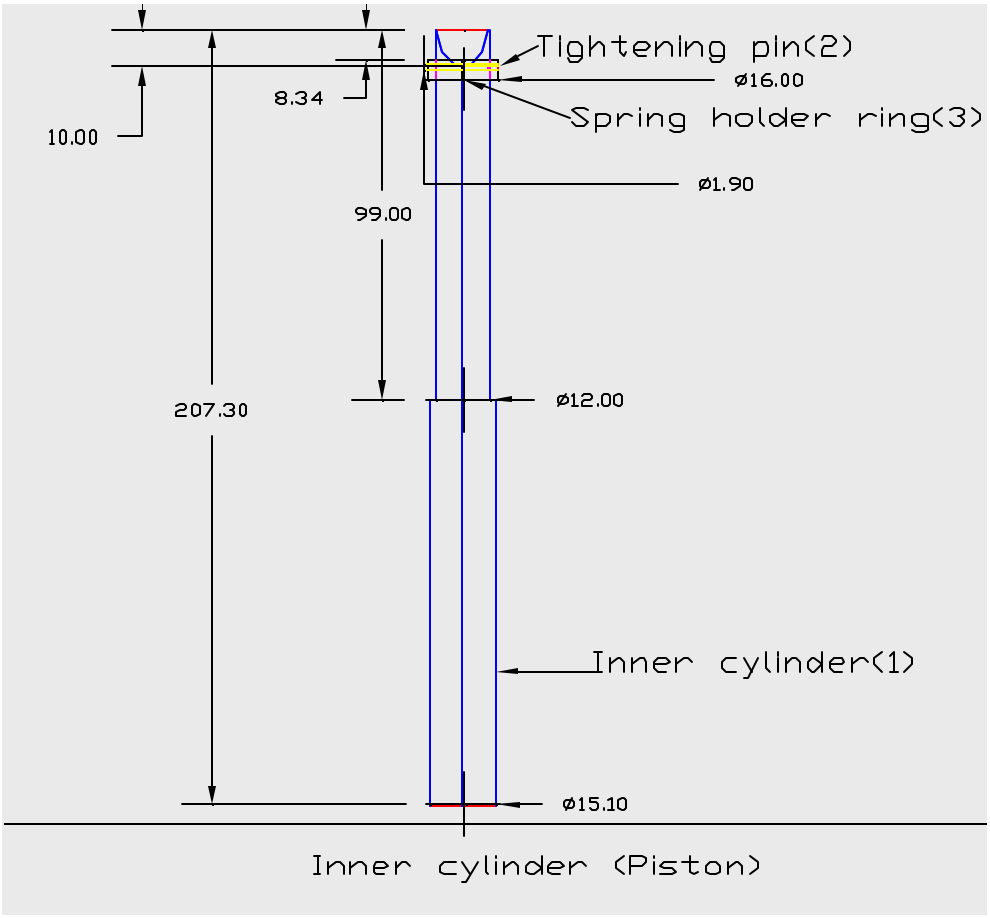

Figure B 3 : Piston dimensions

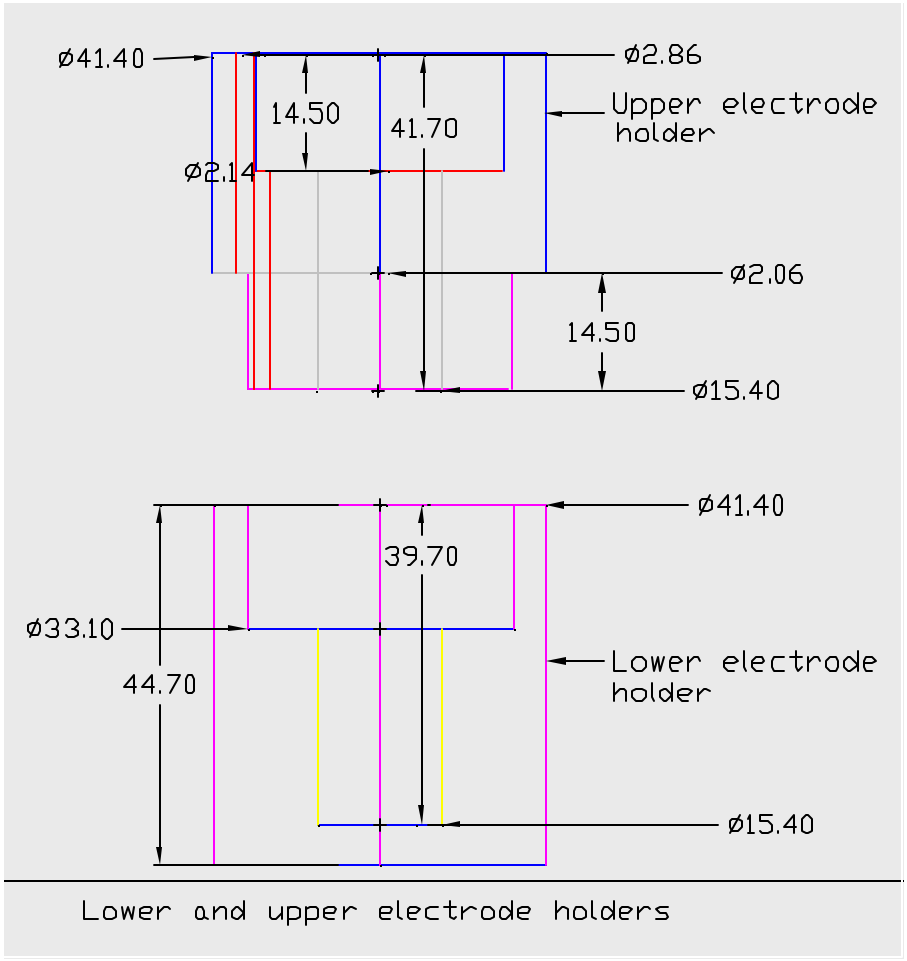

Figure B 4: Electrode holders

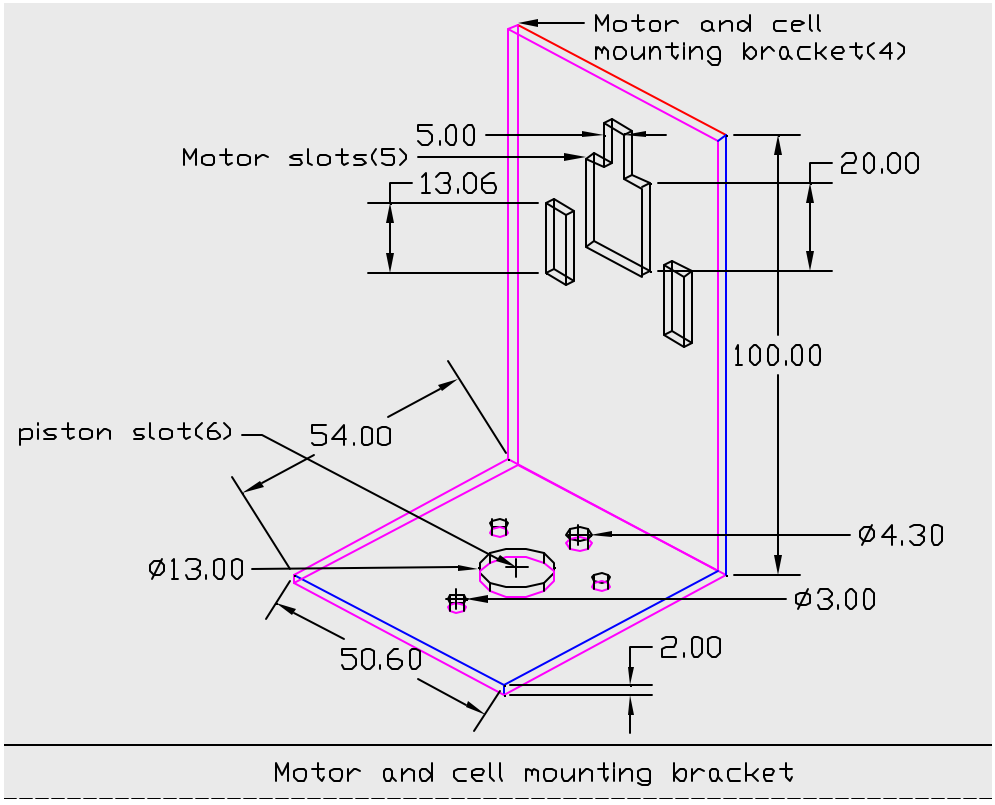

Figure B 5: Motor and cell mounting part dimensions